

Osteoporosis

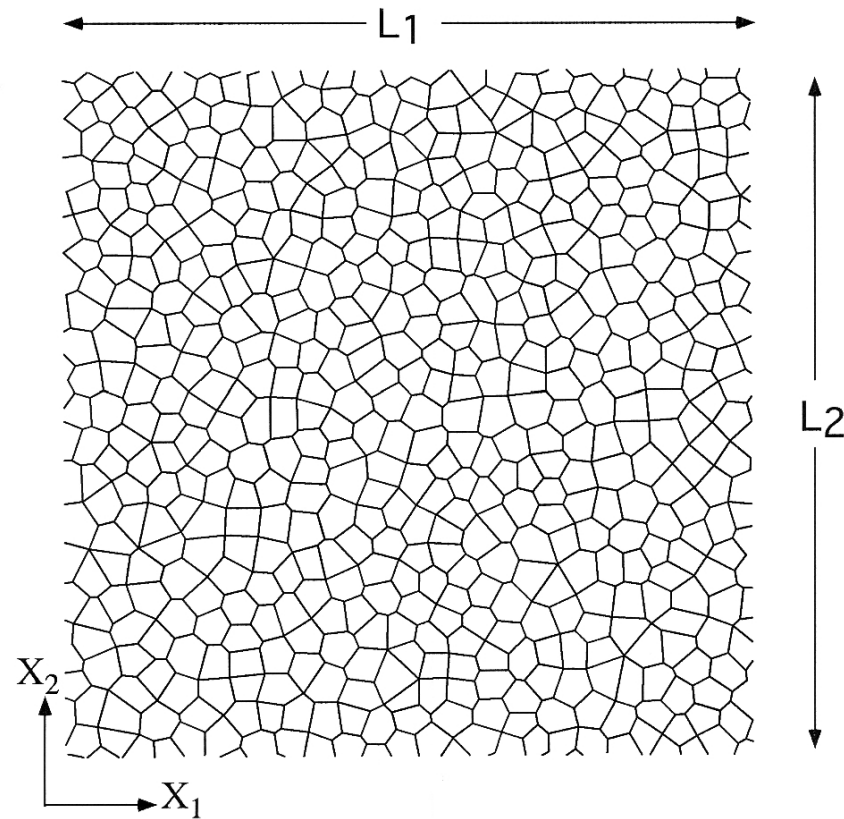
Figure removed due to copyright restrictions. See Figure 1: Vajjhala, S., A. M. Kraynik, et al. "[A Cellular Solid Model for Modulus Reduction due to Resorption of Trabecular Bone.](#)" *Journal of Biomechanical Engineering* 122, no. 5 (2000): 511–15.

- as trabeculae thin - buckling easier $\sigma^* \propto (\rho/\rho_s)^2$
 - once trabeculae begin to resorb, connectivity reduced, strength drops dramatically
 - Modelling
 - can't use unit cell or dimensional analysis (need to model local effects)
 - finite element modelling
 - initially - 2D Voronoi honeycomb
 - 2D representation of vertebral bone } Matt Silva
 - 3D Voronoi foam - Surekha Vajjibala
-

Voronoi honeycomb

- random seed points, draw perpendicular bisectors
- use a minimum separation distance to get cells of approximately uniform size
- FE analysis - each trabecula a beam element
- first calculated elastic moduli
 - FEA results close to analytical model for random (isotropic) honeycomb (40 models, all same ρ^*/ρ_s , about 25x25 cells in each)
 - modulus is average of stiffness over entire material

Modelling: 2D Voronoi

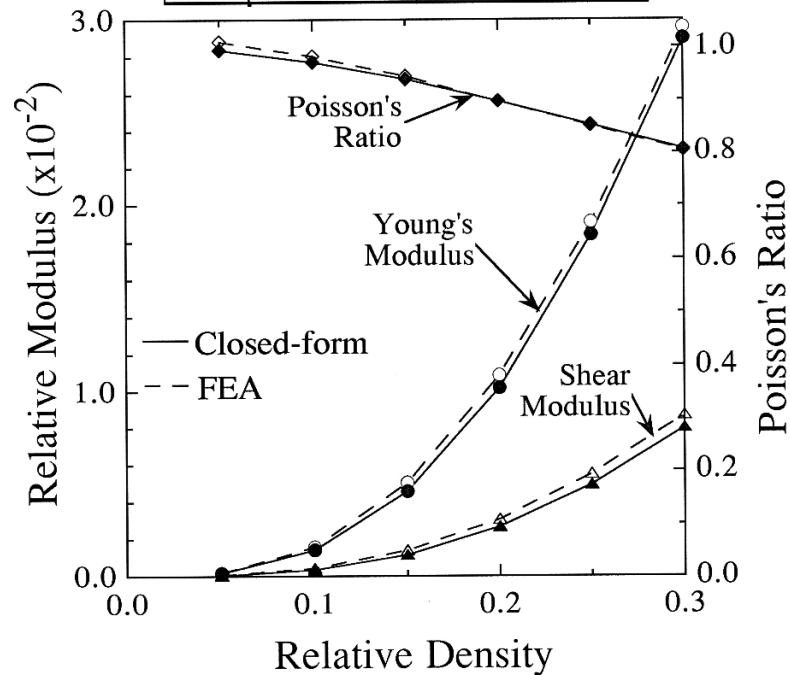


Silva et al, 1995

Source: Silva, M. J., L. J. Gibston, et al. "The Effects of Non-periodic Microstructure on the Elastic Properties of Two-dimensional Cellular Solids." *International Journal of Mechanical Sciences* 37 (1995): 1161-77. Courtesy of Elsevier. Used with permission.

2D Voronoi

E^*/E_s	FEA	$y=0.56x^{2.43}$
E^*/E_s	Equation (1a)	$y=0.63x^{2.54}$
G^*/E_s	FEA	$y=0.18x^{2.53}$
G^*/E_s	Equation (3d)	$y=0.20x^{2.68}$
ν^*	FEA	$y= -1.20x^{1.38} + 1.0$
ν^*	Equation (1b)	$y= -1.30x^{1.55} + 1.0$



Silva et al, 1995

- Next, calculated compressive strength of Voronoi honeycombs
- each cell wall 1-3 beam elements
- Model non-linear elasticity + failure behaviour
- 15x15 cells in model (random seeds \approx isotropic)
- cell wall assumed to be elastic-perfectly plastic $\sigma_{ys}/E_s = 0.01$ $\nu = 0.3$
- for this value of σ_{ys}/E_s , transition between elastic buckling + plastic collapse stress at $\rho^*/\rho_s = 0.035$ in regular hex. honeycomb

- calculated compressive strength of honeycombs with $\rho^*/\rho_s = 0.015, 0.035, 0.05 \neq 0.15$
- generated 5 different Voronoi honeycombs at each ρ^*/ρ_s

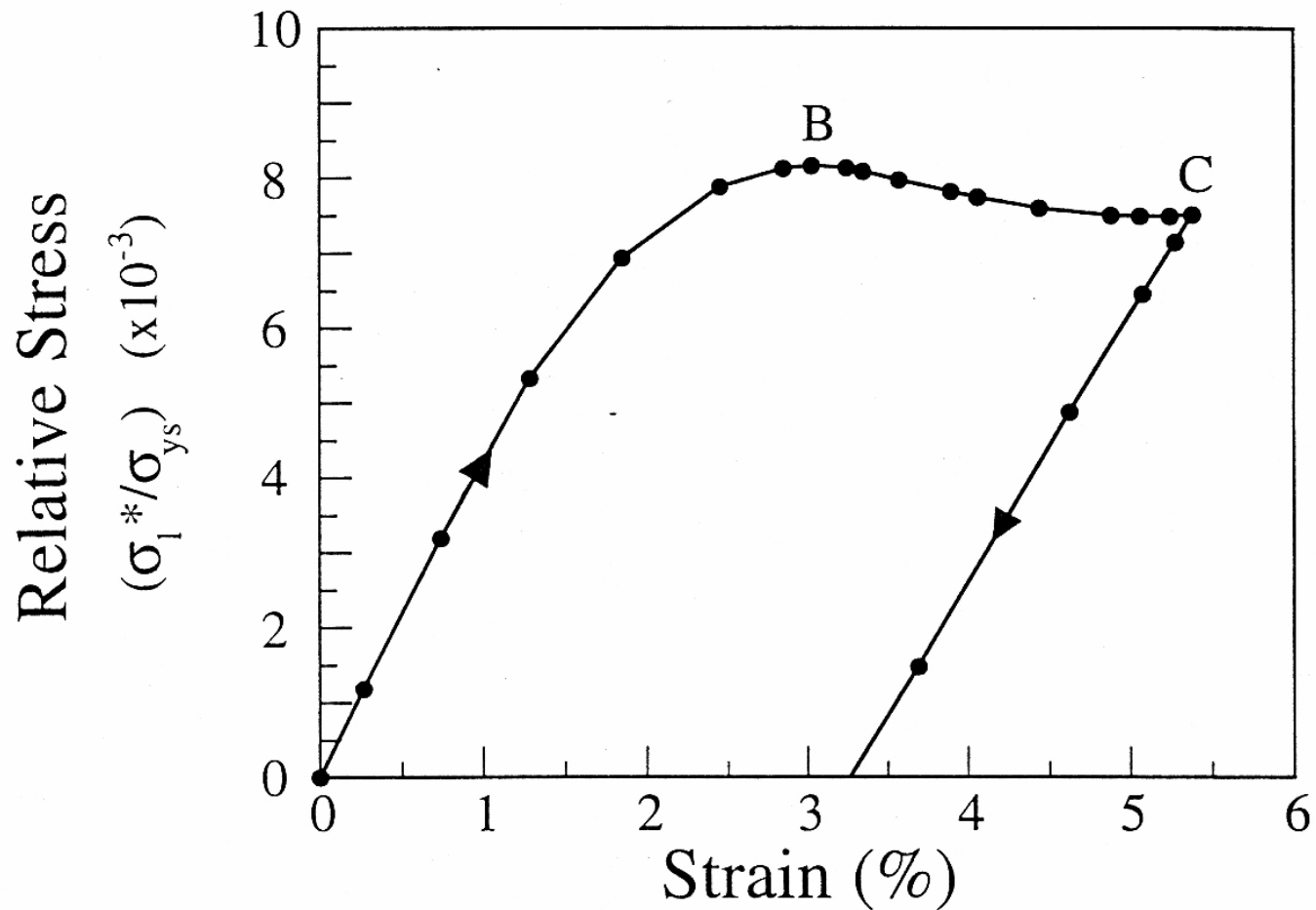
• compressive σ - ϵ behaviour:

$\rho^*/\rho_s \geq 0.05$ - strain softening, permanent defⁿ on unloading
 - plastic hinge formation, cell collapse in narrow localized bands

$\rho^*/\rho_s < 0.035$ - non-linear elastic deformation - recoverable

Strength: 0.6 to 0.8 of $\sigma^*_{periodic}$

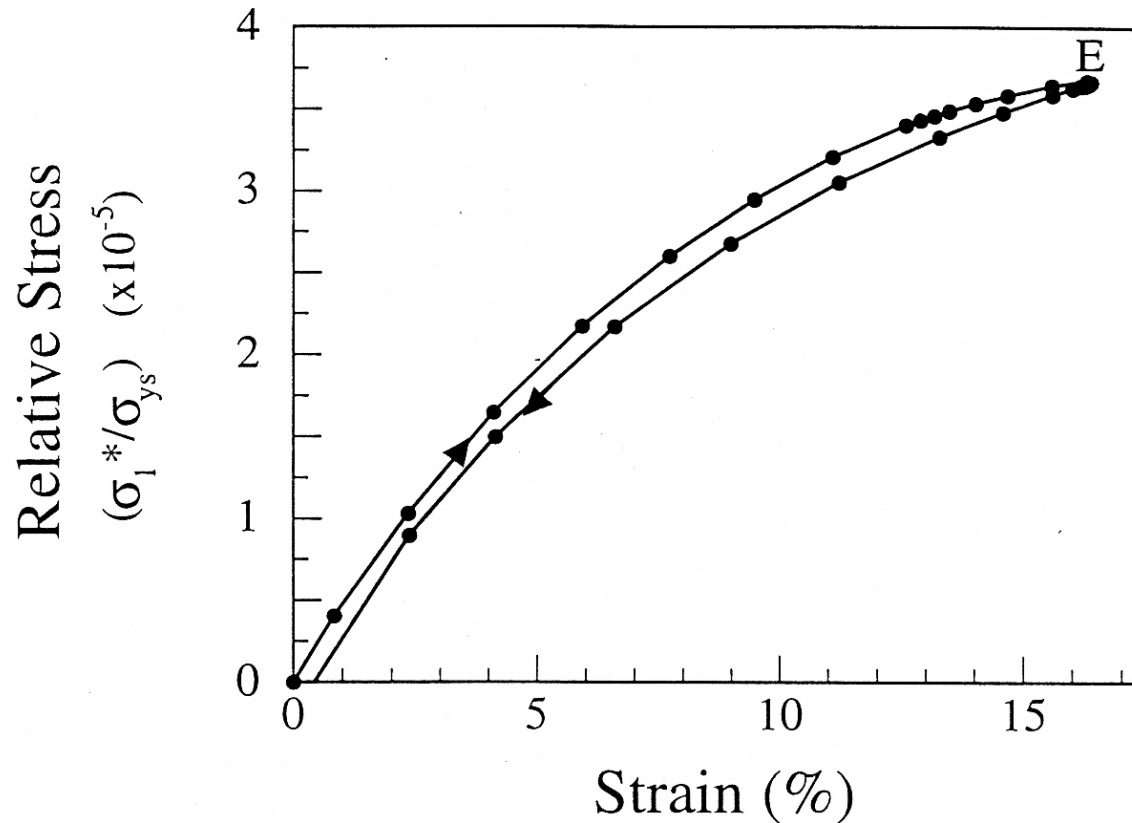
2D Voronoi



Relative density = 15% Plastic failure

Silva et al, 1997

2D Voronoi

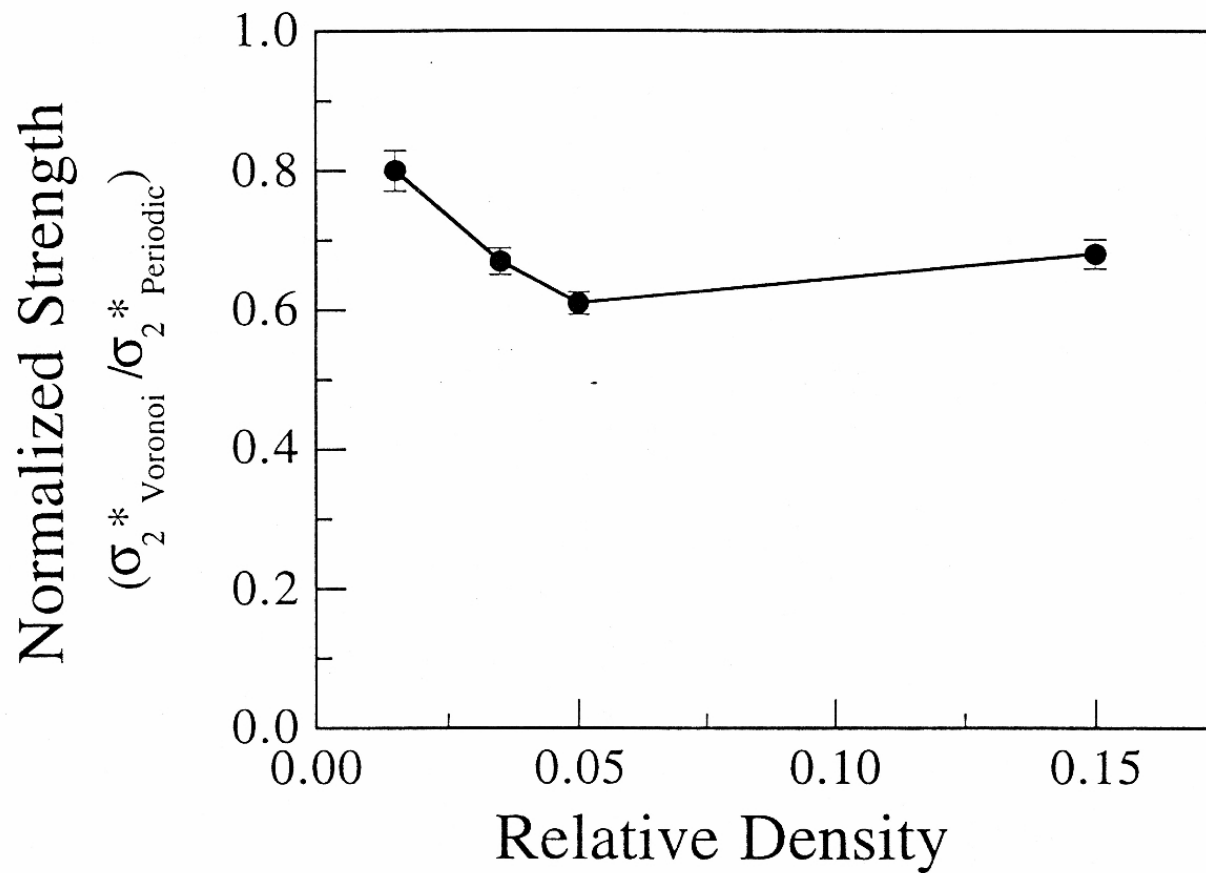


Relative density 1.5%; elastic buckling failure

Silva et al, 1997

Source: Silva, M. J., and L. J. Gibson. "The Effects of Non-periodic Microstructure and Defects on the Compressive Strength of Two-dimensional Cellular Solids." *International Journal of Mechanical Sciences* 39 (1997b): 549-63. Courtesy of Elsevier. Used with permission.

2D Voronoi



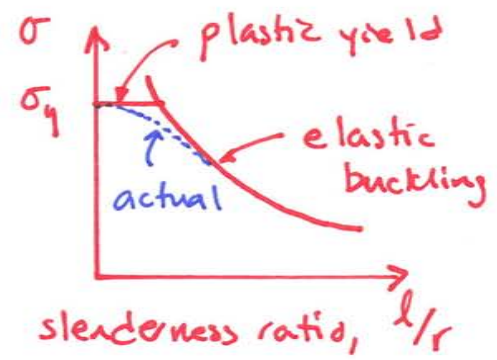
Silva et al, 1997

Source: Silva, M. J., and L. J. Gibson. "The Effects of Non-periodic Microstructure and Defects on the Compressive Strength of Two-dimensional Cellular Solids." *International Journal of Mechanical Sciences* 39 (1997b): 549-63. Courtesy of Elsevier. Used with permission.

- max. normal strains at nodes in honeycombs (linear elastic)
- Voronoi honeycombs - normal distribution
- regular hexagonal honeycombs - dashed lines on plot
- normal strain in vertical cell walls in regular hex. honeycomb \approx mean normal strain in Voronoi
- oblique walls - bending - larger strains
- Voronoi honeycomb 5% of strains outside of range of strain in regular hex. honeycomb

- decrease in strength associated with broader range of strains in Voronoi honeycombs
- minimum strength @ $\rho^*/\rho_s = 0.05$
- interaction between elastic buckling + plastic yield

pin ended column



$$\sigma_{cr} = \frac{\pi^2 E I}{l^2} = \frac{\pi^2 E \pi r^4}{4 l^2 \pi r^2} = \frac{\pi^2}{4} E \left(\frac{r}{l}\right)^2$$

2D Voronoi

Figure removed due to copyright restrictions. See Figure 5; Silva, M. J., and L. J. Gibson. "[The Effects of Non-periodic Microstructure and Defects on the Compressive Strength of Two-dimensional Cellular Solids.](#)" *International Journal Mechanical Sciences* 39, no. 5 (1997): 549-63.

Voronoi Honeycombs - defects

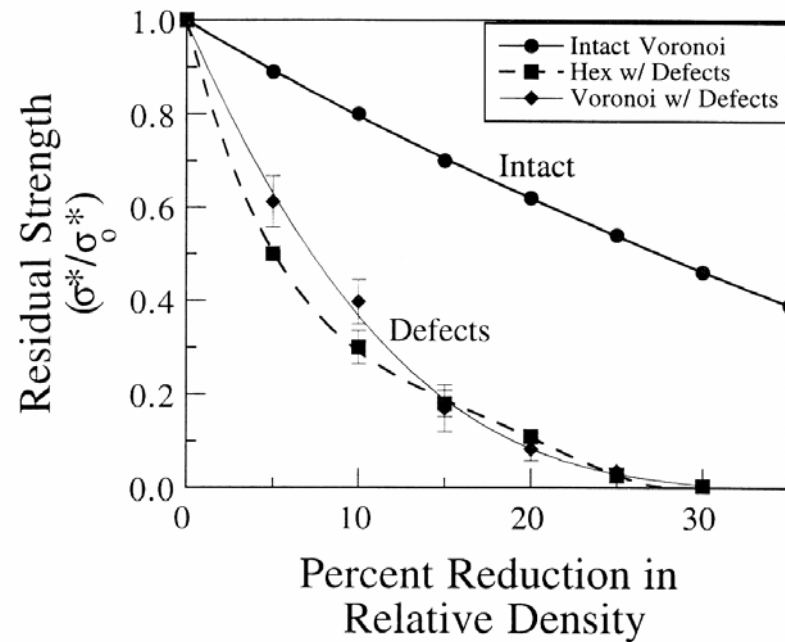
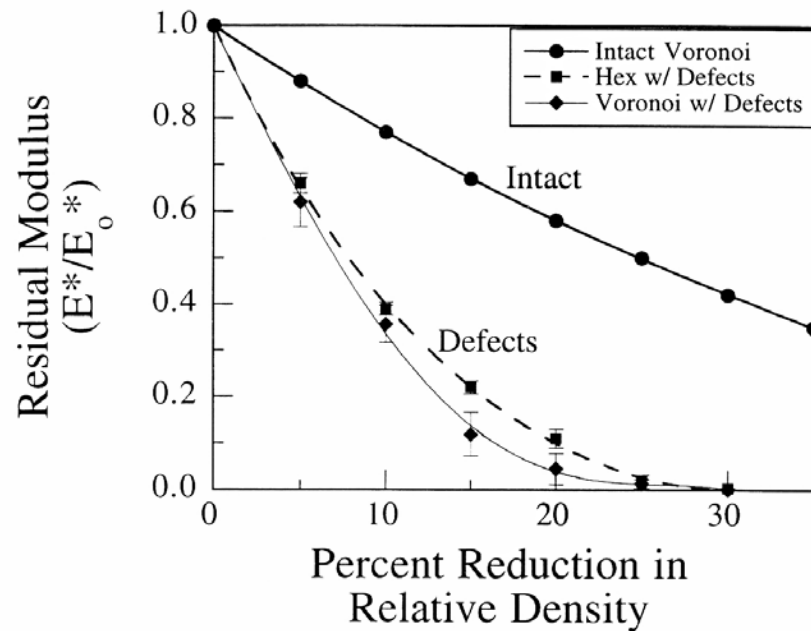
- randomly removed cell walls in both Voronoi + reg. hex. honeycombs
- analyzed both by FEA
- dramatic decrease in modulus + strength, compared with equivalent reduction in density by thinning of cell walls
- $\rho^*/\rho_s = 0.15$ failure by yielding
- $\rho^*/\rho_s = 0.015$ " " elastic buckling

- Modulus + strength reduction similar for Voronoi + reg. hex. honeycombs
- percolation threshold for 2D network hexagonal cells \Rightarrow 55% struts removed

Vertebral trabecular bone - 2D model

- model adapted to reflect trabeculae more aligned in vertical + horizontal directions
- perturbed a square array of struts to get similar orientation of struts as in ^{bone} _{base}
- looked at reduction in number + thickness of longitudinal + transverse struts (independently)

2D Voronoi



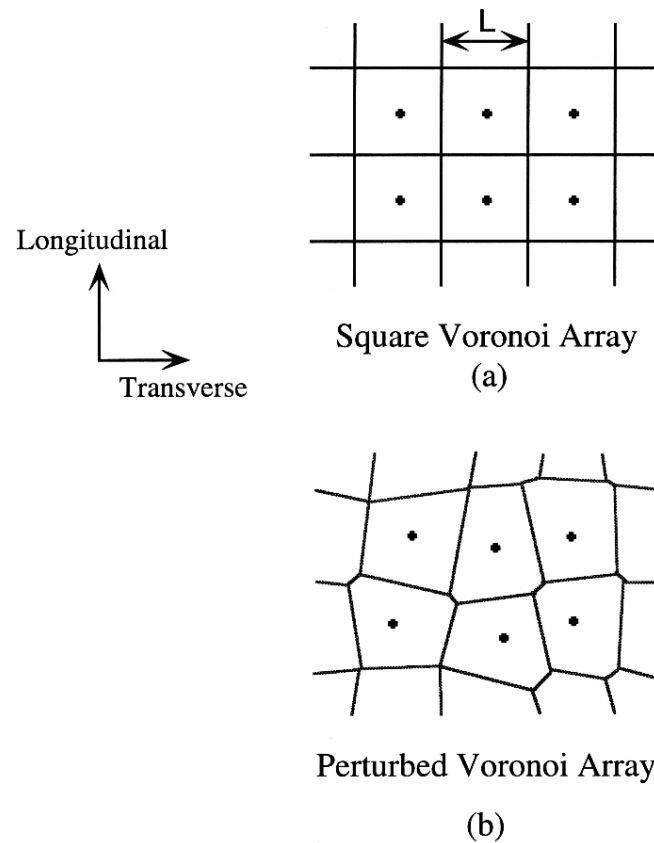
Source: Silva, M. J., and L. J. Gibson. "The Effects of Non-periodic Microstructure and Defects on the Compressive Strength of Two-dimensional Cellular Solids." *International Journal of Mechanical Sciences* 39 (1997b): 549-63. Courtesy of Elsevier. Used with permission.

Silva et al, 1997

2D Voronoi

Figure removed due to copyright restrictions. See Figure 2: Vajjhala, S., A. M. Kraynik, et al. "[A Cellular Solid Model for Modulus Reduction due to Resorption of Trabecular Bone.](#)" *Journal of Biomechanical Engineering* 122, no. 5 (2000): 511–15.

Vertebral Trabecular Bone



Source: Silva, M. J., and L. J. Gibson. "Modelling the Mechanical Behavior of Vertebral Trabecular Bone: Effects of Age-related Changes in Microstructure." *Bone* 21 (1997a): 191-99. Courtesy of Elsevier. Used with permission.

Vertebral Trabecular Bone

Figure removed due to copyright restrictions. See Figure 3: Silva, M. J., and L. J. Gibson. "[Modelling the Mechanical Behavior of Vertebral Trabecular Bone: Effects of Age-related Changes in Microstructure.](#)" *Bone* 21 (1997): 191-99.

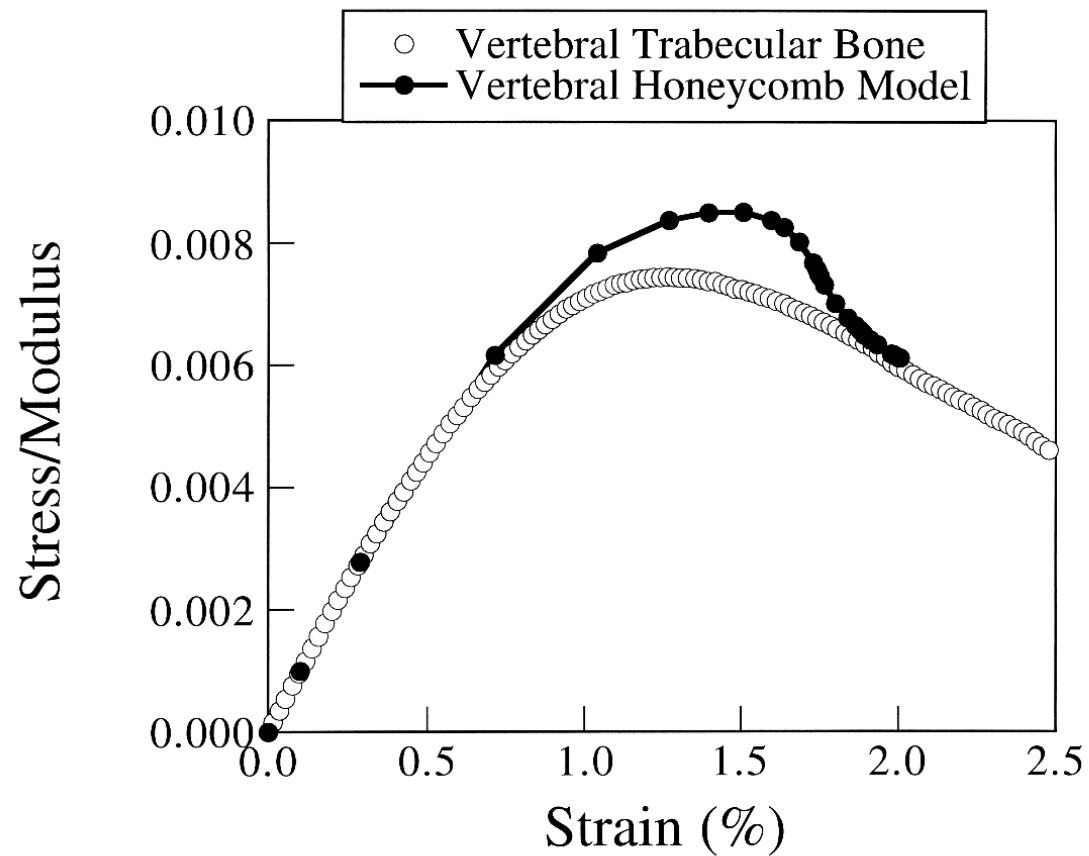
Vertebral Trabecular Bone

Figure removed due to copyright restrictions. See Figure 4: Silva, M. J., and L. J. Gibson. "[Modelling the Mechanical Behavior of Vertebral Trabecular Bone: Effects of Age-related Changes in Microstructure](#)." *Bone* 21 (1997): 191-99.

Vertebral Trabecular Bone

Figure removed due to copyright restrictions. See Figure 5: Silva, M. J., and L. J. Gibson. "[Modelling the Mechanical Behavior of Vertebral Trabecular Bone: Effects of Age-related Changes in Microstructure](#)." *Bone* 21 (1997): 191-99.

Vertebral Trabecular Bone

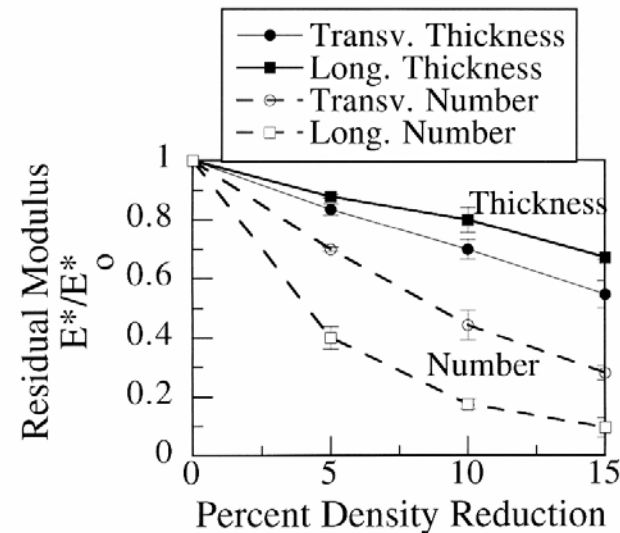


Source: Silva, M. J., and L. J. Gibson. "Modelling the Mechanical Behavior of Vertebral Trabecular Bone: Effects of Age-related Changes in Microstructure." *Bone* 21 (1997a): 191-99. Courtesy of Elsevier. Used with permission.

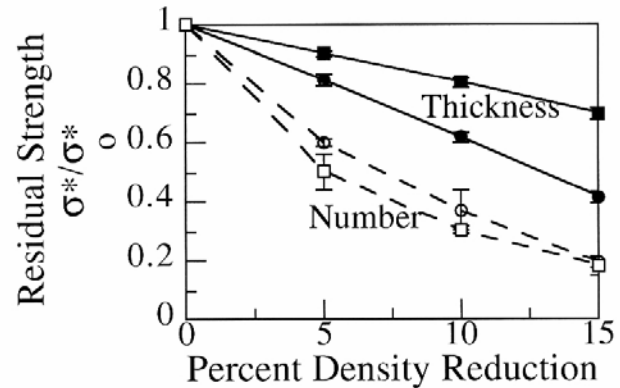
Vertebral Trabecular Bone

Figure removed due to copyright restrictions. See Figure 7: Silva, M. J., and L. J. Gibson. "[Modelling the Mechanical Behavior of Vertebral Trabecular Bone: Effects of Age-related Changes in Microstructure](#)." *Bone* 21 (1997): 191-99.

Vertebral Trabecular Bone



(a)



(b)

Silva et al, 1997

3D Voronoi Model

- same analysis, now with 3D Voronoi Model
 - periodic $3 \times 3 \times 3$ cells, $\rho^*/\rho_s = 0.1$
 - used beam elements, FEA, linear elastic only
 - percolation threshold $\sim 50\%$. struts removed
 - Comparison of 2D + 3D results for modulus: in 3D, modulus reduction more gradual than in 2D
 - also for 2D + 3D - modulus reduction similar for regular + Voronoi structures
-

3D Voronoi Model

Figure removed due to copyright restrictions. See Figure 6: Vajjhala, S., A. M. Kraynik, et al. "[A Cellular Solid Model for Modulus Reduction due to Resorption of Trabecular Bone.](#)" *Journal of Biomechanical Engineering* 122, no. 5 (2000): 511–15.

3D Voronoi Model

Figure removed due to copyright restrictions. See Figure 7: Vajjhala, S., A. M. Kraynik, et al. "[A Cellular Solid Model for Modulus Reduction due to Resorption of Trabecular Bone.](#)" *Journal of Biomechanical Engineering* 122, no. 5 (2000): 511–15.

Metal foams as bone substitute materials

- metals used in orthopaedic implants (eg. hip, knee)
- Co-Cr, Ti, Ta, stainless steel alloys
- biocompatible, corrosion resistant
- but moduli of metals $>$ modulus of bone

e.g. $E_{Ti} = 110 \text{ GPa}$ $E_{cortical} = 18 \text{ GPa}$ $E_{trab.bone} = 0.01 - 2 \text{ GPa}$

- Stress shielding can lead to bone resorption.

- to improve mechanical interaction between implant + bone
 - porous sintered metal beads used to coat implants - promote bone ingrowth
 - also, wire mesh coatings have been developed, primarily for flat implant surfaces
 - recently, interest in using metal foams as coatings
 - longer term, interest in using in replacement vertebral bodies
- variety of processes for making metal foam implant coatings

Metal Foams: Microstructure

Ta, replicating PU foam
with CVD

Ti, replication of PU
foam by slurry infiltration
and sintering

Ti, fugitive phase

Ti, foaming agent

Ti, expansion of Ar gas

Images removed due to copyright restrictions. See Figure 8.1:
Gibson, L. J., M. Ashby, and B. A. Harley. *Cellular Materials in
Nature and Medicine*. Cambridge University Press, 2010.
<http://books.google.com/books?id=AKxiS4AKpyEC&pg=PA228>

Ti, freeze-casting
(freeze-drying)

Ti, selective laser
sintering

Ni-Ti, high temperature
synthesis (powders
mixed, pressed and
ignited by, for example,
tungsten coil heated by
electrical current)

Image sources given in
*Cellular Materials in Nature
and Medicine*

Processing

(a) replicate open cell polyurethane foam

- pyrolyze PU foam \rightarrow 2% dense vitreous carbon
- coat with Ta by CVD \Rightarrow struts 99% Ta, 1% C
- cell size 400-600 μm ; coating thickness 40-60 μm $\rho^*/\rho_s = 0.15-0.25$
- "Trabecular metal" (Zimmer) trade name.
- Ta forms surface oxide Ta_2O_5 - does not bond to bone

- but, if treat with dilute NaOH, then heat to 300°C + cool, then submerge in simulated body fluid (ion conc. matches human blood plasma) \Rightarrow get apatite coating ~~on~~ on foam struts, which bonds to bone

(b) infiltrate slurry of titanium hydride into open cell foam

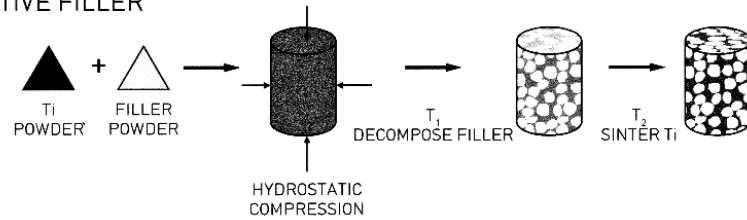
- heat treat to decompose TiH_2
- sinter remaining Ti (also removes initial foam)

(c) fugitive phase methods

- mix TiH_2 powder + fugitive phase powder
- heat to T_1 ($\sim 200^\circ\text{C}$) to decompose filler, then to T_2 (1200°C) to sinter Ti powder

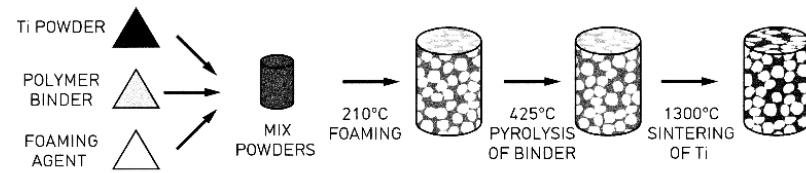
Metal Foams: Processing

FUGITIVE FILLER



(a)

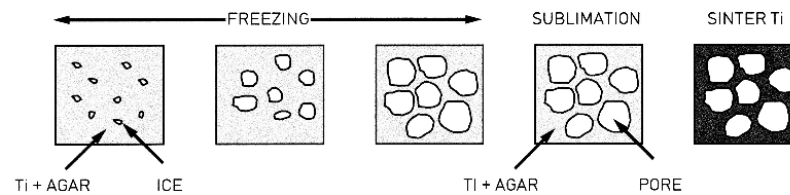
EXPANSION OF A FOAMING AGENT



(b)

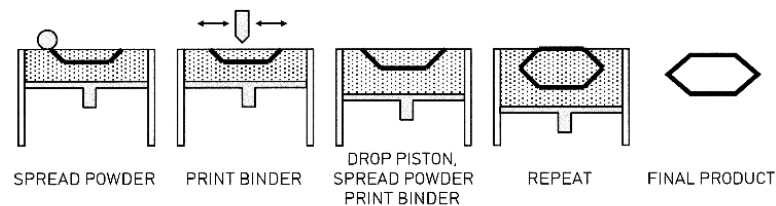
Foaming agent evolves gas at temperature at which polymer is liquid

FREEZE-CASTING



(c)

RAPID PROTOTYPING



(d)

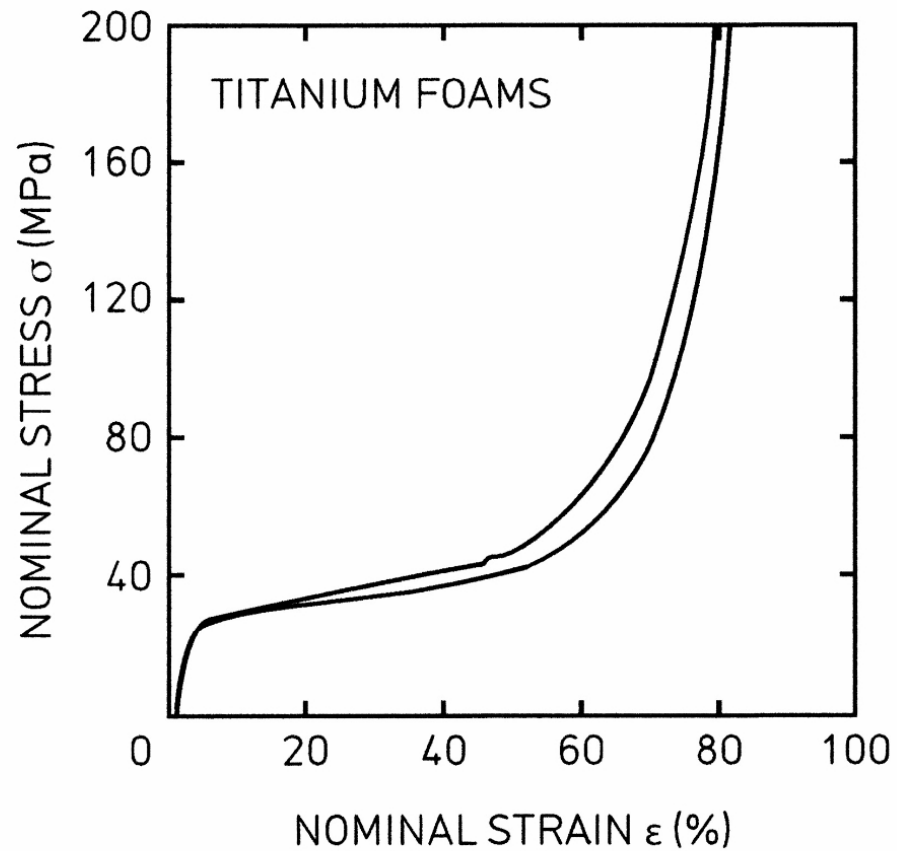
Processes

- (d) expansion of foaming agent
- (e) freeze casting (freeze drying)
- (f) rapid prototyping (3D Printing, selective laser sintering)

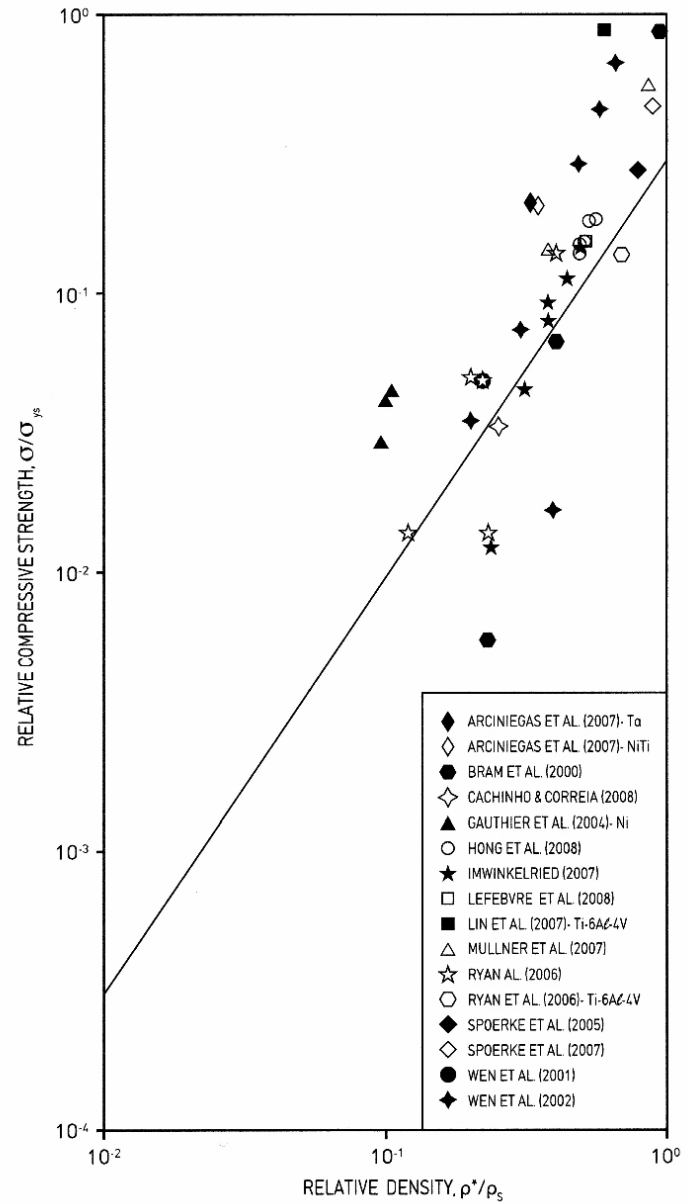
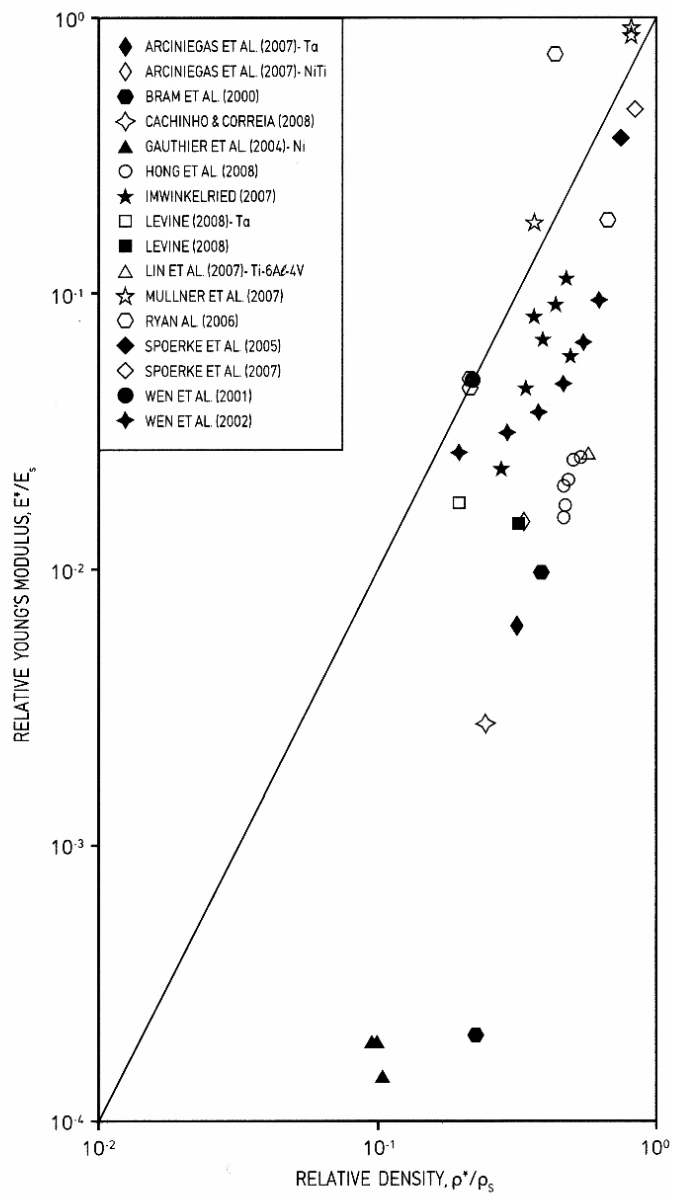
σ - ϵ curves - similar to other foams

data for E^* , σ_c^*

Ti Foam: Stress-strain



Source: Wen, C. E., M. Mabuchi, et al. "Processing of Biocompatible Porous Ti and Mg." *Scripta Materialia* 45 (2001): 1147-53. Courtesy of Elsevier. Used with permission.



Gibson, L. J., M. Ashby, et al. *Cellular Materials in Nature and Medicine*. Cambridge University Press, © 2010. Figures courtesy of Lorna Gibson and Cambridge University Press.

Bone in Evolutionary Studies

Bone structure in evolutionary studies

- phylogenetic chart - big picture - structural biomaterials (mineralized)
 - sponges - first multi celled animal
 - calcarea: CaCO_3 spicules (needles)
 - hexactinellida: SiO_2 - "glass sponges"
 - demospongiae: most sponges - some have SiO_2 spicules
 - spongin (type of collagen)
-
- cnidarians - eq. corals, jellyfish
 - corals CaCO_3
 - mollusca - bivalves, snails, octopus
 - if mineralized CaCO_3
 - arthropods eq. hexapoda (insects), arachnida (spiders), crustaceans (shrimp, lobster)
 - exoskeleton of insects + spiders: chitin
 - crustaceans: chitin may be mineralized with CaCO_3

Vertebrates

- cyclostomata - jawless fish - lampreys hagfish
 - no vertebra - notochord
 - no bone
 - chondrichthyes - sharks, rays, skates
 - cartilaginous skeleton - some mineralization, but not true bone
 - actinopterygii - ray finned fish
 - true bone
 - 450 million years ago (MYA)
-

Bone structure + loading

- bone grows in response to loading
- bone structure reflects mechanical loading + function e.g. quadruped vs biped
- evolutionary studies have looked at trabecular bone architecture + density.

METAZOA

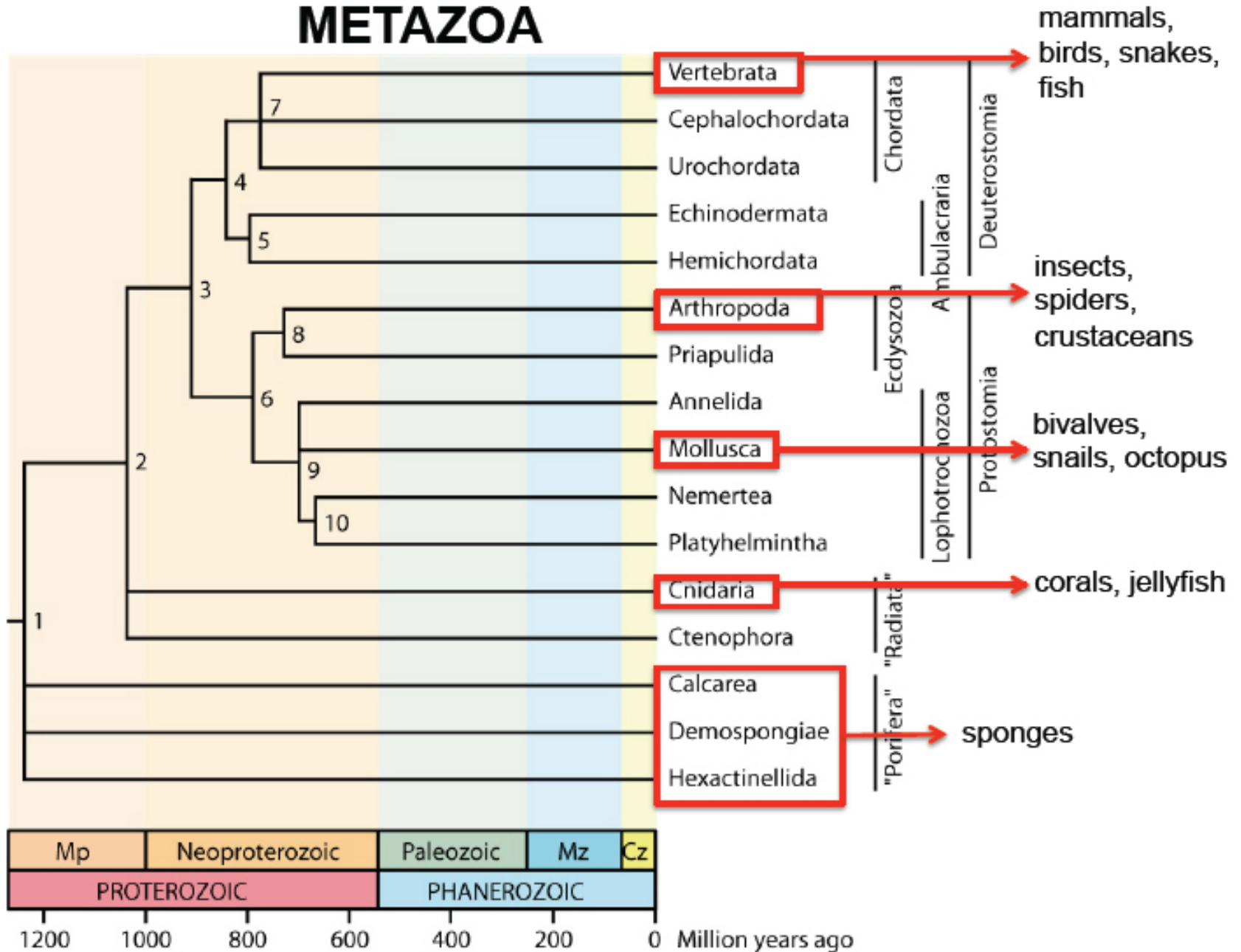


Fig. 2 A timetree of metazoan phyla. Divergence times are shown in Table 1. Abbreviations: Cz (Cenozoic), Mp (Mesoproterozoic), and Mz (Mesozoic).

Hedges and Kumar, 2009

From: *The Timetree of Life*. Hedges, S. B., and S. Kumar (eds.) © 2009 Oxford University Press. All rights reserved. This content is excluded from our Creative Commons license. For more information, see <http://ocw.mit.edu/help/faq-fair-use/>.



Venus Flower Basket (*Euplectella aspergillum*)

- Hierarchical structure
- Remarkably stiff, tough
- Joanna Aizenberg (Harvard)
- Aizenberg et al (2004) Biological glass fibers: correlation between optical and structural properties. PNAS

VERTEBRATA

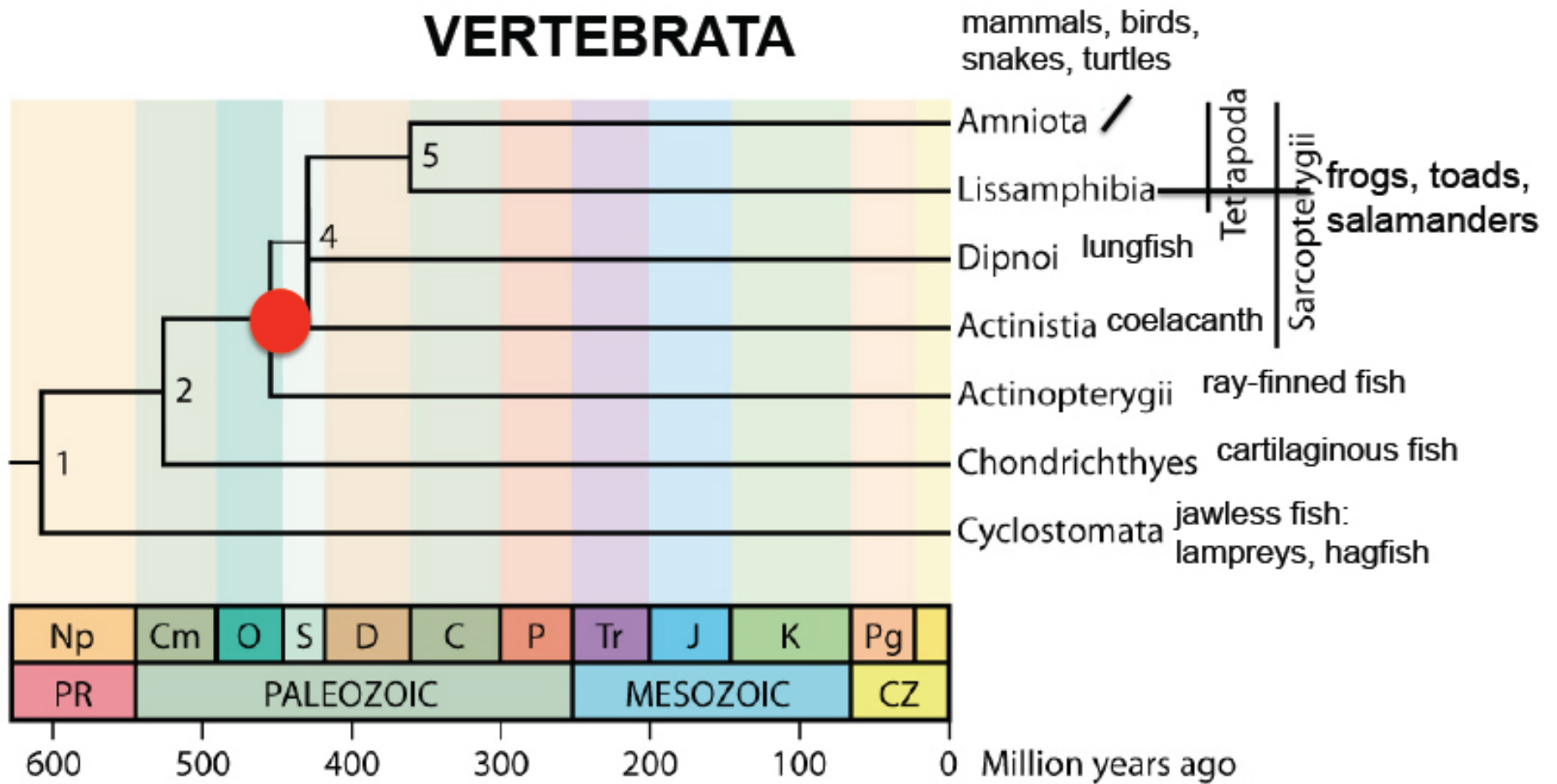


Fig. 2 A timetree of vertebrates. Times of divergence are averages of estimates from different studies listed in Table 1. Abbreviations: C (Carboniferous), Cm (Cambrian), CZ (Cenozoic), D (Devonian), J (Jurassic), K (Cretaceous), Np (Neoproterozoic), O (Ordovician), P (Permian), Pg (Paleogene), PR (Proterozoic), S (Silurian), and Tr (Triassic).



Common ancestor of all boned vertebrates roughly 450 MYA

(Hagfish video)

From: *The Timetree of Life*. Hedges, S. B., and S. Kumar (eds.) © 2009 Oxford University Press. All rights reserved. This content is excluded from our Creative Commons license. For more information, see <http://ocw.mit.edu/help/faq-fair-use/>.

Trabecular bone studies in human evolution

Oreopithecus bambolii (Rook et al, 1999)

- 7-9 MYA late Miocene hominid, found in Italy
- quadruped or biped?
- compared trabecular architecture in ilium in apes, O. bambolii, humans
- only had 2 fragments of ilium - left + right
- took radiographs of both + digitally reconstructed a single ilium

Comparisons

- (a) posterosuperior margin - marginal handles thicker than apes
- (b) antero superior margin - iib bundle relatively structured compared to apes
- (c) antero inferior margin - well developed a-i spine not seen in apes
- (d) supra acetabular area - high density region
- Collectively, observations suggest O. bambolii trab. architecture in ilium more similar to humans than apes
- suggests habitual bipedal locomotion (humans - obligatory bipeds)

anatomy of the human pelvis

anatomical diagrams

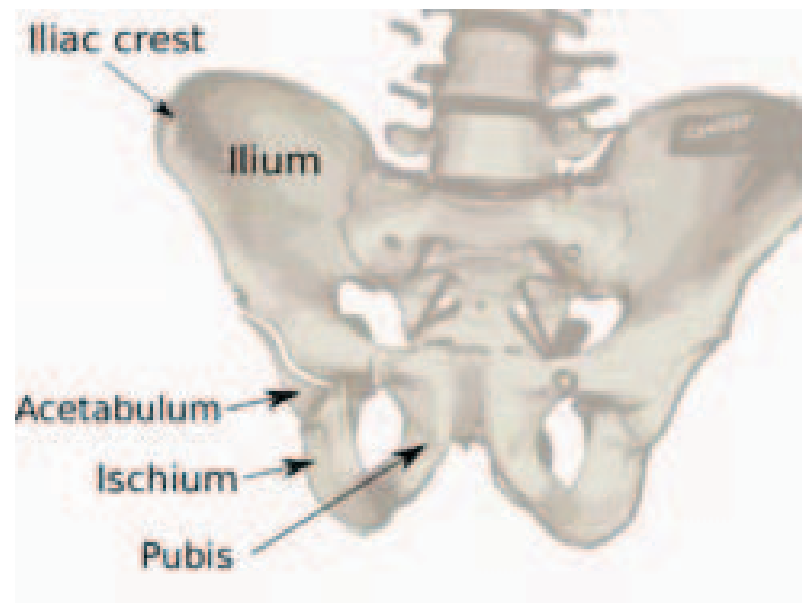


Image is in the public domain. Source: [Wikimedia Commons](#).

anatomical diagrams

Trabecular architecture: Ilium

Figure removed due to copyright restrictions. See Figure 1: Rook L., et al. "[Oreopithecus was a Bipedal Ape after All.](#)" *Proceedings of the Natural Academy of Sciences* 96 (1999): 8795-99.

Digitally reconstructed ilium

Figure removed due to copyright restrictions. See Figure 2: Rook L., et al. "[Oreopithecus was a Bipedal Ape after All.](#)" *Proceedings of the Natural Academy of Sciences* 96 (1999): 8795-99.

Comparison of trabecular architecture

Figure removed due to copyright restrictions. See Figure 3: Rook L., et al. "[Oreopithecus was a Bipedal Ape after All.](#)" *Proceedings of the Natural Academy of Sciences* 96 (1999): 8795-99.

MIT OpenCourseWare
<http://ocw.mit.edu>

3.054 / 3.36 Cellular Solids: Structure, Properties and Applications
Spring 2015

For information about citing these materials or our Terms of Use, visit: <http://ocw.mit.edu/terms>.